# Combustible Gas Cylinder Detonation
# upon Incident Shock Focusing

## P. Yu. Georgievskiy[a], V. A. Levin[a], and O. G. Sutyrin[a]*

*[a] Institute of Mechanics of Moscow State University, Moscow, 119192 Russia*
**e-mail: sutyrin@imec.msu.ru*

Two-dimensional interaction of a shock in air with elliptic area (two-dimensional gas bubble) filled with propane-oxygen mixture with addition of heavy gas is numerically studied using Euler's equations. Propane combustion is modeled with one-stage Arrhenius kinetics. Three different ignition regimes are found: direct detonation initiation by sufficiently strong shock, detonation near the triple point formed during weaker shock refraction and detonation at the focusing point of even weaker shock. The latter regime is observed only for significantly elongated bubbles. Detonation initiation regime dependence on shock Mach number and bubble diameter ratio is determined. It is shown that due to bubble elongation, critical Mach number may be significantly lowered in comparison with direct initiation.

**Keywords:** shock wave, gas bubble, shock-bubble interaction, shock focusing, cumulation, gas detonation, combustion.

Interaction of shock waves with local inhomogeneities takes place in many flows ranging from cosmic processes with supernovae to high-speed combustion systems and inertial confinement fusion. Such flows are commonly studied on the basis of shock-bubble interaction (SBI) and reactive shock-bubble interaction (RSBI) that include a wide range of shock wave effects, instability types and reaction wave types. Starting with first experiments [1], RSBI is actively researched in latest years. Recent numerical simulations [2–4] have revealed importance of initial pressure and incident shock strength in terms of determining resulting ignition type—deflagration of detonation—as well as significant mixing reduction caused by reaction front propagation.

For shock-gas bubble interaction, several key flow features are known: uneven bubble acceleration and distortion, vorticity deposition, turbulent gas mixing and transversal shock focusing. The latter is of special interest regarding combustion initiation, and thus this effect also receives additional interest in recent years. It is known that all main flow parameters—incident shock intensity, bubble density, and initial bubble shape—play important role in determining shock refraction patterns and resulting focusing intensity [5]. In general, more elongated bubble shapes result in internal shock focusing pattern (Type-I, [6]), in which transversal shock focusing is more intense than in external ones (Type-II) and, not less importantly, the highest pressures and temperatures are reached inside the distorted bubble. The similar effect is observed during interaction of a shock with local fine dust cloud [7].

Based on these data, the bubble shape may as well be assumed to play an important role in combustion initiation of the mixture through incident shock refraction and focusing.

In the present work, an interaction of a shock with elliptic reactive gas bubble is numerically studied in two-dimensional plane formulation.

The unsteady prefect gas mixture flows are modeled using Euler's equations:

$$\frac{\partial}{\partial t}\begin{pmatrix} \rho_i \\ \rho u \\ \rho v \\ H - p \end{pmatrix} + \frac{\partial}{\partial x}\begin{pmatrix} \rho_i u \\ p + \rho u^2 \\ \rho u v \\ Hu \end{pmatrix} + \frac{\partial}{\partial y}\begin{pmatrix} \rho_i v \\ \rho u v \\ p + \rho v^2 \\ Hv \end{pmatrix} = 0,$$

where $\rho_i$ are gas component densities, $\rho = \sum \rho_i$ is total mixture density, $u, v$ are velocity components along Cartesian axes $x, y$, respectively, while pressure $p$ ant total enthalpy per gas volume unit $H$ are calculated as follows:

$$p = \sum \rho_i \frac{R}{\mu_i} T, \quad H = \sum \rho_i (c_{pi} T + h_{0i}).$$

Here, $T$ is absolute temperature, $R$ is universal gas constant, and $\mu_i$, $c_{pi}$, $h_{0i}$ are component molar masses,
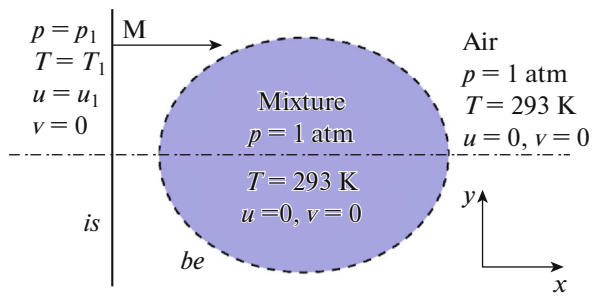
**Fig. 1.** Initial condition outline: *is*—incident shock, *be*—bubble (gas cylinder) edge. The dot-and-dash line denotes the symmetry plane of the problem.

specific heat capacities, and heats of formation, respectively.

Thermodynamic parameters for six gas components used ($C_3H_8$, $O_2$, $N_2$, $CO_2$, $H_2O$, Xe) are given in [8]. Propane combustion reaction is modeled with one-stage Arrhenius kinetics [9].

A "MUSCLE"-type finite-volume method with linear value reconstruction at cell interfaces, van Leer limiter and HLLC Riemann solver that ensures second-order solution approximation in both time and space is applied for numerical simulation. Uniform square computational grid with 12 μm cell size is used so that detonation wave reaction zone is resolved with 5−6 cells.

Initial condition for the problem is given in Fig. 1. The shock wave propagates from left to right through still air (1 part $O_2$, 4 parts $N_2$ by volume) that contains an elliptic area filled with stoichiometric flammable gas mixture (1 part $C_3H_8$, 5 parts $O_2$, 5 parts $N_2$, 15 parts Xe by volume) under normal conditions. Mixture density is 3.1 times greater than density of surrounding air which ensures the attainability of internal shock focusing pattern [5].

Uniform gas state behind the shock is governed by Mach number $M$ using Rankine−Hugoniot conditions. Cylinder cross-section geometry is determined by ellipse diameter ratio $\eta = d_x/d_y$, with constant section area of 12.6 cm$^2$ corresponding to round cylinder ($\eta = 1$) with 4 cm diameter.
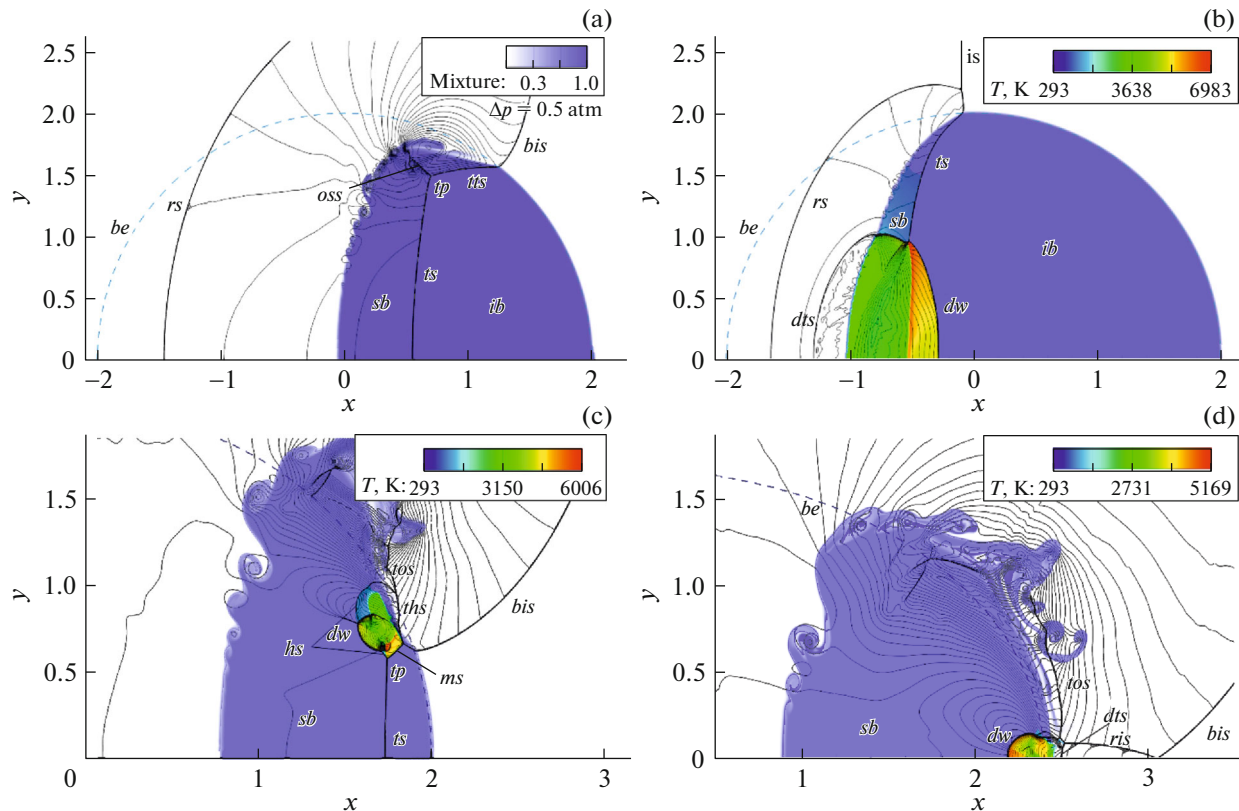


**Fig. 2.** Shock refraction (a) and different gas mixture detonation initiation regimes: (b) direct at $M = 3.4$; (c) upon shock refraction, M = 3.0; (d) upon shock focusing, $M = 2.7$, $\eta = 1.44$. Only the upper half of the flow is shown; pressure contours, and colors represent reactive mixture mass fraction and gas temperature (only for $T > 1100$ K). *ib*, *sb* are undisturbed and shocked parts of the bubble; *bis* is convex part of the incident shock; *rs*, *ts*—reflected and transmitted shocks; *tts*, *oss* are transversal secondary shocks; *tp* is triple point; *dw* is detonation wave; *ms* is Mach stem; *hs* is heat release-induced shocks; *ris* is *bis*-shock reflected off the symmetry plane; *dts*—detonation induced shock wave in air; *tos*, *ths*— transmitted shock waves *oss* and *hs*, respectively.
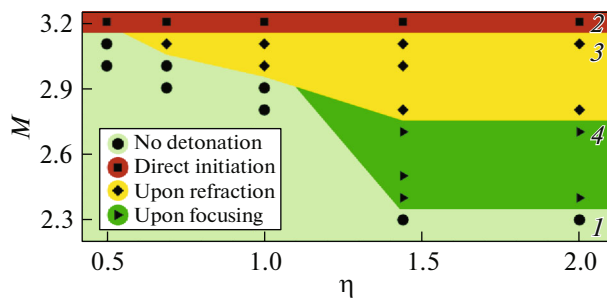
**Fig. 3.** Ignition regime dependence on Mach number $M$ and bubble diameter ratio η. Each symbol represents single simulation, some intermediate values are omitted. Circle on green—no detonation, square on red—direct initiation, diamond on yellow—detonation upon shock refraction, triangle on green—detonation upon shock focusing.

Due to transmitted shock *ts* falling behind the incident shock *is* (Fig. 2a), transversal shocks *tts*, *oss* and triple point *tp* form inside the bubble and propagate diagonally toward the symmetry plane. Depending on flow parameters, triple point *tp* and shock *tts* reach the plane outside or inside the bubble [5, 6] and sharp pressure and temperature rise is observed in the local area. Based on these data, at least three different bubble detonation ignition regimes may be expected to exist: direct mixture detonation initiation by strong enough shock, ignition near the triple point *tp* for lower shock Mach number and ignition in the focusing area of even weaker shock.

In the performed simulations, direct detonation initiation is observed at $M \geq 3.2$. Detonation wave *dw* (Fig. 2b) forms near the left bubble edge shortly after shock transition into the mixture, overtakes the *ts* shock and propagate further in Chapman–Jouguet regime, fully consuming the reactive mixture. Typical cellular structure with approximately 0.5 mm cell width is observed on detonation wave front.

For lower Mach numbers, the temperature behind the transmitted shock *ts* is insufficient for direct mixture ignition. During the shock refraction, an area of intense heat release forms near the triple point *tp* and generates *hs* and *ths* shocks that propagate in mixture and in air outside of the bubble, respectively. During the interaction of *hs* shock with secondary shock inside the bubble, self-sustaining detonation wave *dw* forms (Fig. 2c) and then propagates through the whole deformed bubble.

For even weaker shocks ($M \leq 2.9$), the heat release near the triple point is insufficient and no detonation is observed for round bubbles. Although for elongated bubbles (η > 1) detonation initiation is observed due to focusing of transversal shocks and triple points in the reactive mixture near the right bubble pole (Fig. 2d).

Based on performed parametric study for $2.0 \leq M \leq 3.5$ and $0.5 \leq \eta \leq 2.0$, detonation initiation regime dependence on these parameters may be qualitatively estimated (Fig. 3). Only direct initiation at $M \geq 3.2$ is

observed for flattened bubbles (η = 0.5). With increase of η, non-direct initiation regimes appear, at first near triple point for η = 0.7 and then at shock focusing for η = 1.44. During that, the critical Mach number sufficient for detonation decreases by about 35%: from $M = 3.2$ to $M = 2.4$. No significant changes are observed with further bubble elongation.

Based on numerical simulation of interaction of a shock with elliptic area—a bubble—of reactive gas mixture, the detonation initiation regime and critical incident shock intensity are shown to significantly depend on bubble shape. The applied model does not include viscosity, heat transfer and diffusion effects as well as induction time of combustion reaction, and thus the bounds of parameters ranges corresponding to specific ignition regimes are determined only approximately. Although the main effect, i.e., the significant reduction of critical Mach number with bubble elongation, may probably be considered to have the real foundation. This effect, in particular, may be applied for efficiency increase of direct-flow high-speed combustion systems with burning induced by interaction of fuel jet with oblique stationary shock.

## CONFLICT OF INTEREST

Authors declare that they have no conflict of interest.

## REFERENCES

1. N. Haehn, D. Ranjan, C. Weber, J. Oakley, D. Rothamer, and R. Bonazza, Combust. Flame **159**, 1339 (2012).

2. F. Diegelmann, V. Tritschler, S. Hickel, and N. Adams, Combust. Flame **163**, 414 (2016).

3. F. Diegelmann, S. Hickel, and N. Adams, Combust. Flame **174**, 85 (2016).

4. F. Diegelmann, S. Hickel, and N. Adams, Combust. Flame **181**, 300 (2017).

5. P. Yu. Georgievskiy, V. A. Levin, and O. G. Sutyrin, Shock Waves **25**, 357 (2015).

6. J. Ray, R. Samtaney, and N. Zabusky, Phys. Fluids **12**, 707 (2000).

7. P. Yu. Georgievskii, V. A. Levin, and O. G. Sutyrin, Tech. Phys. Lett. **42**, 936 (2016).

8. *Thermodynamic Tables* (Thermodynamic Res. Center Texas, A&M Univ., College Station, TX, 1998).

9. C. Westbrook and F. Dryer, Prog. Energy Combust. Sci. **10**, 1 (1984).